Optimized Pulse Sequences at High Field

Oliver Speck

Medical Physics, Dept. of Diagnostic Radiology, University Hospital Freiburg,
Hugstetter Str. 55, 79106 Freiburg, Germany

1. Introduction

The increasing interest in MRI at high magnetic field (i.e. 3T and above) has mainly been driven by neuro-imaging applications. More specifically, the higher sensitivity to detect activations in functional neuro-imaging studies was a main incentive.

With the more widespread availability of high field systems many other applications benefit from the main advantage of higher magnetic fields: the improved signal to noise ratio. Since MRI is an inherently low signal modality, disadvantages of high field systems, e.g. increased RF-power deposition, are tolerated but need to be addressed.

Apart from technical challenges to build high field systems with sufficient B0 homogeneity over a large FOV, high temporal stability, and especially RF-coils with homogeneous excitation profile, physical properties of tissue and RF-waves change with increasing field strength. Therefore, even if many of the engineering problems can be solved now or in the future, MR imaging sequences need to be adapted for the use at high field strength.

In this article, the field strength dependence of fundamental properties and effects that are important for MRI are reviewed. A step-by-step description for the numerical prediction of MR signals of arbitrary pulse sequences is given, which allow optimizing MR sequences based on the knowledge about changes of the physical properties of tissue. Field strength related problems and solutions of selected imaging sequences are demonstrated. Finally, adjustment procedures are examined with respect to field strength related effects.

2. Field-strength dependent parameters

If sample noise dominates as is the case for human in vivo measurements, the sensitivity increases almost linearly with field strength. This is due to the very small value of the Boltzmann exponent that determines the magnetization of a sample. This can be approximated by a linear function. Various experimental studies have confirmed this behavior. Unfortunately, other properties change with increasing field strength and thus frequency. Many of these change to the disadvantage of high field. In tissue, the spin-lattice relaxation time T_1 increases while the spin-spin relaxation time T_2 is relatively constant or slightly reduced (depending on the measurement method) and T_2^* decreases due to the increased local field variation [1-3]. To compensate for this, obviously longer repetition and shorter echo times are required.

A dominant effect of higher field strength is the increased RF power deposition and the reduced spatial homogeneity of the RF amplitude generated by volume transmit-coils. The power deposition was long assumed to increase quadratically with frequency. However, newer theoretical and experimental work has shown that the increase is lower at frequencies over 200 MHz [4]. Nevertheless, SAR restrictions are a main limiting factor at high field strength and have to be considered in the sequence design. In addition, the RF-field inhomogeneity, which is caused by the short wavelength in human tissue relative to the body extent, requires sequences that are insensitive to flip angle variations and extensive intensity correction [5].

The increased frequency dispersion, which is of advantage for spectroscopic applications, also implies that off-resonance related imaging properties, e.g. the chemical shift of fat or dephasing effects in steady state sequences, increase with field strength. In order to keep the artifact level comparable and to account for the shorter T_2, higher imaging bandwidth is needed. Correspondingly, the image noise increases proportional to the square root of the bandwidth partially annihilating the SNR gain. On the other hand this allows acquiring more signals, e.g. more slices in the same TR. However, this simple adaptation to higher field strength is not always possible, e.g. in situations, were the gradient strength or peripheral nerve stimulation limit the bandwidth as in EPI.

3. Numerical signal prediction

The temporal evolution of magnetization under the influence of RF-pulses, imaging gradients, local field distortions and relaxation is described by the Bloch equation. In compact form it can be written as:

$$\frac{d}{dt}\vec{M} = \gamma\, \vec{M} \times \vec{B} - R(\vec{M} - \vec{M}_0) \tag{1}$$

where:

$$\vec{M} = \begin{pmatrix} M_x \\ M_y \\ M_z \end{pmatrix};\ \vec{B} = \begin{pmatrix} B_x \\ B_y \\ B_z \end{pmatrix};\ R = \begin{pmatrix} 1/T_2 & 0 & 0 \\ 0 & 1/T_2 & 0 \\ 0 & 0 & 1/T_1 \end{pmatrix};\ \vec{M}_0 = \begin{pmatrix} 0 \\ 0 \\ M_0 \end{pmatrix}. \tag{2}$$

It is convenient and common to describe magnetization in a coordinate system rotating around the z-axis with a frequency corresponding to the Larmor frequency:

$$\omega_0 = \gamma\, B_0\,. \tag{3}$$

If B_0 points into the z-direction, the Bloch equation in the rotating coordinate system takes the form:

$$\frac{d}{dt}\vec{M} = \gamma\, \vec{M} \times (\vec{B} - \vec{B}_0) - R(\vec{M} - \vec{M}_0)\,. \tag{4}$$

The solution of the first part is given by a rotation of the magnetization, while the second part leads to exponential relaxation towards the equilibrium value. The temporal evolution of magnetization that satisfies this equation can be given in a closed form for special cases. It can be divided into various parts corresponding to certain time intervals in an MR sequence.

If no RF-pulse is applied, magnetization rotates around the z-axis according to the local field $\vec{B} - \vec{B}_0$ resulting in dephasing of so called off-resonance magnetization:

$$\vec{M}(t) = \Re_z(\phi)\,\vec{M}(0) = \begin{pmatrix} \cos\phi & -\sin\phi & 0 \\ \sin\phi & \cos\phi & 0 \\ 0 & 0 & 1 \end{pmatrix} \vec{M}(0), \text{ with } \phi = \gamma(\vec{B} - \vec{B}_0)t\,. \tag{5}$$

During an on-resonant RF-pulse $\vec{B}$, magnetization rotates around the axis given by the pulse phase. For a pulse along x this leads to:

$$\vec{M}(t) = \Re_x(\alpha)\,\vec{M}(0) = \begin{pmatrix} 1 & 0 & 0 \\ 0 & \cos\alpha & -\sin\alpha \\ 0 & \sin\alpha & \cos\alpha \end{pmatrix} \vec{M}(0), \text{ with } \alpha = \gamma \vec{B}_x t\,. \tag{6}$$

For other pulse phases, the corresponding rotation matrix needs to be calculated. In case of off-resonance excitation, the resulting effective B-field in the rotating frame is no longer within the transversal plane but has a z-component and is given by:

$$\vec{B} = \begin{pmatrix} B_x \\ B_y \\ B_z - \omega_{RF} / \gamma \end{pmatrix}. \tag{7}$$

Thus the corresponding rotation matrix needs to be calculated around this effective axis. During all times, the magnetization is subject to relaxation. The solution of the Bloch equation for the case $\vec{B} = 0$ can be given as follows:

$$\vec{M}(t) = \begin{pmatrix} E_2 & 0 & 0 \\ 0 & E_2 & 0 \\ 0 & 0 & E_1 \end{pmatrix} \vec{M}(0) + (1 - E_1)\vec{M}_0 \text{, with } E_{1,2} = \exp(-t / T_{1,2}) \text{ .} \tag{8}$$

The evolution of magnetization during any pulse sequence can be calculated by piecewise integration and thus application of the transformations given above. Time periods with varying conditions, e.g. during the application of amplitude or frequency modulated RF-pulses, can be calculated with very high accuracy using the hard pulse approximation, i.e. by subdividing the pulse into short time periods of constant amplitude and frequency.

Using this framework, it is possible to include the effects of selective pulses during a gradient by calculation of the magnetization for different locations in gradient direction resulting in the corresponding slice shape. Similarly, the consequences of RF-amplitude and phase variations within the imaging volume can be predicted if the RF-field distribution is known.

More complex effects, e.g. flow, motion, diffusion, or magnetization transfer can be included to result in a more realistic description of the MR experiment.

4. Specific MR-sequences

The field strength dependent properties of tissue and RF-fields put certain requirements on MR sequences used at higher fields. The sequence weighting has to be adopted to result in the desired contrast for the range of T_1 and T_2 times in the tissue under investigation. Ideally, the sequence should maintain its signal intensity and contrast even under conditions of inhomogeneous RF-fields that result in varying effective flip angles over the field of view. Finally, the sequence has to meet the SAR restrictions without major loss of efficiency.

For a number of basic MR-sequences, the flip angles dependence of the signal intensity can be calculated easily (Fig. 1). For EPI or gradient echo sequences with TR>T_1, the flip angle dependency is given by $\sin(\alpha)$, while for a spin echo signal the refocusing pulse leads to a $\sin^2(\frac{\alpha}{2})$ dependency (for the excitation an extra $\sin(\alpha_{ex})$ is introduced). For fast gradient echoes the plot is scaled to the signal intensity at the Ernst angle and leads to a flip angle dependency that is largely independent of T_1. For the static pseudo steady state of TSE the signal has a very moderate dependence on the flip angle. However, overall SAR is the highest for this sequence due to the large number of refocusing pulses.

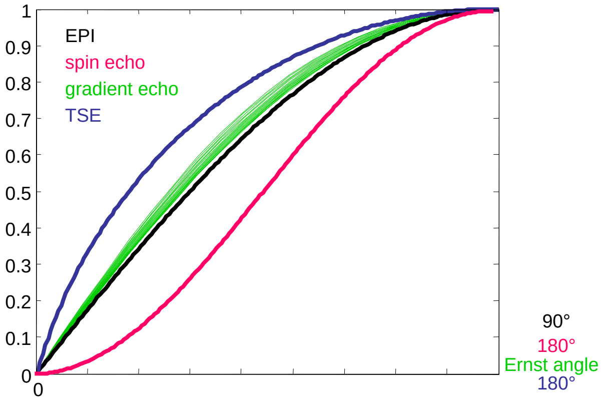

Fig. 1: The flip angle dependence of different sequences. The plot axes are scaled to the optimum flip angle for each method. The TSE sequence shows the lowest flip angle dependence and the spin echo the strongest, which is even stronger when the excitation pulse is considered, too.

In the following a few selected sequences are discussed and possible solutions for their application at high field strength are shown.

T_2-Imaginig

As shown above, the TSE sequence has benign properties with regard to flip angle variation. It is also very insensitive to local B_0-field variation, making it a perfect candidate for high field imaging. However, the high SAR often prevents its usage at high field without reducing the flip angle and thus signal. A solution to this problem is the introduction of variable flip angles throughout the echo train leading to the formation of the so called Hyperecho [6, 7]. With this modification, the SAR can be reduced dramatically without loss of signal intensity and with only minor changes in the point spread function.

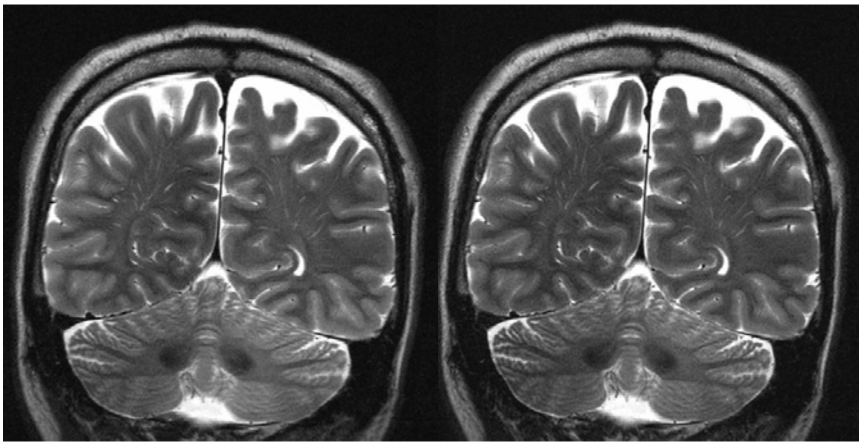

Fig. 2: TSE image (left) acquired at 4T with conventional refocusing pulses (180°) and Hyper-TSE image (right) with refocusing flip angles varying down to 60° resulting in an SAR reduction of 72%.

T_1-Imaging

Although spin echo methods are sensitive to RF field inhomogeneities, they are often the preferred choice for T_1 weighted imaging in the brain, especially for the detection of contrast agent. With longer and converging T1 times of the tissue, the contrast diminishes at high field. In addition, strong magnetization transfer effects lead to further contrast reduction. For detailed anatomic volumetric measurements with high resolution, 3D magnetization prepared fast gradient echo methods are frequently used. With these methods spatially varying signal intensity and contrast are a major problem at high field. By the optimization of the pulses and flip angles applied, the effects of varying flip angles can be compensated and a homogeneous intensity and contrast can be obtained [8].

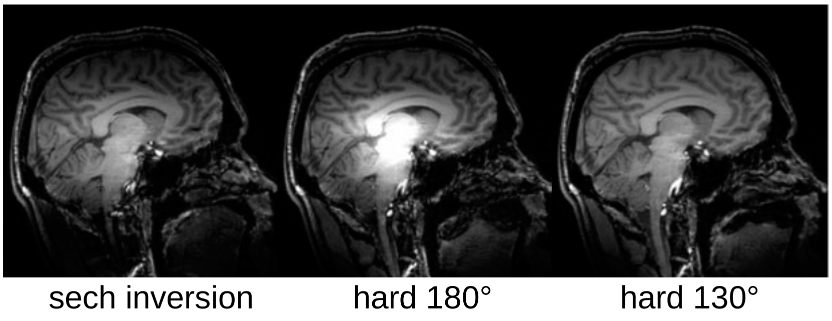

Fig. 3: MDEFT image acquired at 4.7T with different implementations of the inversion pulse. The hard 130° inversion compensates for much of the signal inhomogeneities. (Courtesy of R. Deichmann, London, UK)

Echo Planar Imaging

Many high field applications in the brain, e.g. fMRI, pMRI, or DTI, rely on echo planar imaging. While SAR and flip angle dependence are minor issues, the increased local field variations cause markedly increased geometric image distortions and signal loss. Geometric distortions can be as large as a few centimeter and are frequently ignored leading to potential misinterpretations of anatomic locations. This local shift Δxp is mainly in phase encoding direction and given by the frequency offset $\Delta\omega$ and the effective bandwidth in this direction $1/Np\,Esp$ (number of points in phase direction times echo spacing):

$$\Delta xp = \Delta\omega\, Np\, Esp\, xp_{res}\,. \tag{9}$$

Corrections are either image-based using non-linear deformation relative to a geometrically correct data set [9] or based on measurements of the local image distortion [10] by field or point-spread-function maps [11, 12].

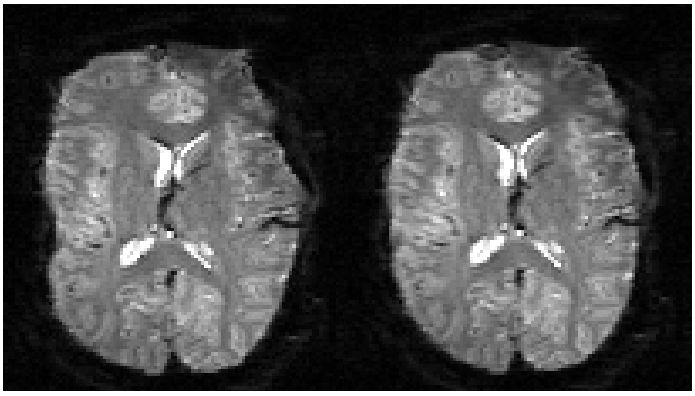

Fig. 4: GE-EPI image acquired at 3T with 2mm resolution. On the left, the uncorrected image with phase encoding in left-right direction. On the right, the image corrected with the PSF method.

Signal loss is caused by intra-voxel dephasing during the long readout and echo time especially of GE-EPI. Methods proposed for compensation include z-shimming [13], compensation gradients [14], and reduction of voxel size [15]. While z-shimming is very effective it increases the measurement time since multiple acquisitions are necessary. The use of compensation gradients improves the signal at the cost of other more homogeneous regions. Finally, thinner slices, which have shown to reduce the signal loss, require more slices to be acquired.

Many imaging methods can benefit from accelerated imaging schemes, e.g. partial Fourier imaging or partial parallel imaging, with regard to SAR and artifact behavior. However, since the total RF-deposition for a sequence is reduced by reducing the scan time, the average RF-deposition is only reduced if the next sequence has significantly lower SAR or if a pause is inserted between measurements reducing overall efficiency.

5. System adjustments

Before an MRI measurement can be performed, the system needs to be adjusted according to the properties of the object to be examined. The center transmit and reception frequency is simply determined from a global or local free induction decay. The frequency adjustment is reliable even at very high field strength.

Assuming sufficiently homogeneous main magnetic fields, the relative field deviation caused by the probe or subject is independent of the field strength. However, the absolute inhomogeneity should be kept at a comparable level in order to fully benefit from the increased signal and frequency dispersion. Therefore, shimming becomes increasingly important and stronger shim coils with higher spatial selectivity (higher order shims) are required, which are also more difficult to adjust.

For a volume coil at low field strength, the goal of the transmitter adjustment is well defined, e.g. a 90° pulse should maximize the received FID signal or minimize the remaining z-magnetization. At higher frequencies the B1-field amplitude varies considerably across the object. Thus, the task is to define the parameter to be optimized. Maximizing the total signal will yield flip angles, which are higher than desired in the center of the object. In addition, for cross coil operation, the reception profile will interact with the B1-homogeneity of the transmit coil and change the adjusted transmit voltage.

6. Conclusion

MR imaging at high field of 3 and 4T has been very successful over the past few years and many of the obstacles that were thought to be prohibitive of high field imaging have been overcome by technical developments of the system hardware and sequence optimization. The large degree of freedom in the design of MR sequences has certainly not yet been fully exploited and further optimizations are likely. However, the very high field range of 7T and higher is still vastly unexplored land. The main focus of the development has been on hardware and while many of the solutions developed for 3T will also be applicable to higher field, the increasing problem of RF field inhomogeneity seems to be the major obstacle. Most applications have so far only aimed at relatively small sub-regions of the brain with limited volume coverage. It is unlikely that the physics of RF wave propagation will change and thus new concepts, e.g. parallel transmission [16], need to be developed to overcome this fundamental limitation.

7. References

1. Norris, D.G., *High field human imaging.* J Magn Reson Imaging, 2003. **18**(5): p. 519-29.
2. Hennig, J., et al., *Functional magnetic resonance imaging: a review of methodological aspects and clinical applications.* J Magn Reson Imaging, 2003. **18**(1): p. 1-15.
3. Stanisz, G.J., et al., *T1, T2 relaxation and magnetization transfer in tissue at 3T.* Magn Reson Med, 2005. **54**(3): p. 507-12.
4. Vaughan, J.T., et al., *7T vs. 4T: RF power, homogeneity, and signal-to-noise comparison in head images.* Magn Reson Med, 2001. **46**(1): p. 24-30.
5. Hoult, D.I. and D. Phil, *Sensitivity and power deposition in a high-field imaging experiment.* J Magn Reson Imaging, 2000. **12**(1): p. 46-67.
6. Hennig, J. and K. Scheffler, *Hyperechoes.* Magn Reson Med, 2001. **46**(1): p. 6-12.
7. Hennig, J., M. Weigel, and K. Scheffler, *Multiecho sequences with variable refocusing flip angles: optimization of signal behavior using smooth transitions between pseudo steady states (TRAPS).* Magn Reson Med, 2003. **49**(3): p. 527-35.
8. Thomas, D.L., et al., *3D MDEFT imaging of the human brain at 4.7 T with reduced sensitivity to radiofrequency inhomogeneity.* Magn Reson Med, 2005. **53**(6): p. 1452-8.
9. Otte, M., *Elastic registration of fMRI data using Bezier-spline transformations.* IEEE Trans Med Imaging, 2001. **20**(3): p. 193-206.
10. Jezzard, P. and R.S. Balaban, *Correction for geometric distortion in echo planar images from B0 field variations.* Magn Reson Med, 1995. **34**(1): p. 65-73.
11. Zaitsev, M., J. Hennig, and O. Speck, *Point spread function mapping with parallel imaging techniques and high acceleration factors: fast, robust, and flexible method for echo-planar imaging distortion correction.* Magn Reson Med, 2004. **52**(5): p. 1156-66.
12. Zeng, H. and R.T. Constable, *Image distortion correction in EPI: comparison of field mapping with point spread function mapping.* Magn Reson Med, 2002. **48**(1): p. 137-46.
13. Glover, G.H., *3D z-shim method for reduction of susceptibility effects in BOLD fMRI.* Magn Reson Med, 1999. **42**(2): p. 290-9.
14. Posse, S., et al., *Single-shot T(2)* mapping with 3D compensation of local susceptibility gradients in multiple regions.* Neuroimage, 2003. **18**(2): p. 390-400.
15. Merboldt, K.D., J. Finsterbusch, and J. Frahm, *Reducing inhomogeneity artifacts in functional MRI of human brain activation-thin sections vs gradient compensation.* J Magn Reson, 2000. **145**(2): p. 184-91.
16. Katscher, U., et al., *Transmit SENSE.* Magn Reson Med, 2003. **49**(1): p. 144-50.